

Properties of the Clinoptilolite: Characterization and Adsorption Tests with Methylene Blue

*Original*

Properties of the Clinoptilolite: Characterization and Adsorption Tests with Methylene Blue / Dosa, Melodj; Piumetti, Marco; Bensaid, Samir; Russo, Nunzio; Baglieri, Orazio; Miglietta, Fabrizio; Fino, Debora. - In: JOURNAL OF ADVANCED CATALYSIS SCIENCE AND TECHNOLOGY. - ISSN 2408-9834. - ELETTRONICO. - 5:1(2018), pp. 1-10. [10.15379/2408-9834.2018.05.01.01]

*Availability:*

This version is available at: 11583/2714063 since: 2018-09-27T16:01:08Z

*Publisher:*

Cosmos Scholars Publishing House

*Published*

DOI:10.15379/2408-9834.2018.05.01.01

*Terms of use:*

This article is made available under terms and conditions as specified in the corresponding bibliographic description in the repository

*Publisher copyright*

default\_article\_editorial [DA NON USARE]

-

(Article begins on next page)

# Properties of the Clinoptilolite: Characterization and Adsorption Tests with Methylene Blue

Melodj Dosa<sup>1</sup>, Marco Piumetti<sup>1,\*</sup>, Samir Bensaid<sup>1</sup>, Nunzio Russo<sup>1</sup>, Orazio Baglieri<sup>2</sup>, Fabrizio Miglietta<sup>2</sup> and Debora Fino<sup>1</sup>

<sup>1</sup>Department of Applied Science and Technology, Politecnico di Torino, Corso Duca degli Abruzzi 24, 10129 Turin, Italy

<sup>2</sup>Department of Environment, Land and Infrastructure Engineering, Politecnico di Torino, Corso Duca degli Abruzzi 24, 10129 Turin, Italy

**Abstract:** In this work, the physico-chemical properties of clinoptilolite (a natural zeolite) were analyzed by complementary techniques including X-ray diffractogram, N<sub>2</sub> physisorption at -196 °C, FESEM and EDX analysis. Zeolite is classified as a mesoporous material (cavities ≈ 15 nm) with a specific surface area of 36 m<sup>2</sup>g<sup>-1</sup>. The porous size distribution shows a peak in the mesoporous region. This zeolite is characterized by anhedral particles assembled on top of one another: this is a characteristic of material growth by magma with impurities (Mordenite) in the pores. The presence of impurities was evidenced with EDX analysis (Fe=0.68% at, Mg=0.47% at.). Then, the adsorption tests were performed with two solutions of methylene blue (MB) at different concentrations (namely 250 and 500 mgL<sup>-1</sup>). The results showed that the adsorption of the dye is more efficient in the case of 250 mg L<sup>-1</sup> concentration, with an abatement of 96% after 2h. The abatement corresponding to the higher concentration of MB is about 92.5% after 2h. The kinetic order of MB on clinoptilolite was calculated. The results suggest a second order reaction. In the future, clinoptilolite will be studied for the abatement of metal ion solutions in order to be used as a molecular sieve in the waste water treatment field.

**Keywords:** Clinoptilolite, Natural Zeolite, Waste water treatment, Dyes, Methylene blue adsorption.

## 1. INTRODUCTION

In recent years, natural and synthetic zeolites have become very interesting study materials for various different applications [1-6]. Their story began about 260 years ago, when Axel F. Cronstedt discovered a mineral, in a copper mine in Sweden, with an interesting characteristic: it seemed to boil up when it was heated. Because of this property, Cronstedt named this mineral “zeolite” which translates from the Greek meaning “boiling stone” [7]. Following this discovery, interest towards zeolites increased but only in the XX century did it become possible to obtain a clear resolution of their crystal structure [8-10]. Thanks to these studies, scientists were able to highlight the main characteristic of these solids [11]:

- There is a tridimensional framework characterized by [SiO<sub>4</sub>] and [AlO<sub>4</sub>] tetrahedra;
- The zeolites are composed of regular channels and micropores with different shapes and sizes;
- The micropores contain adsorbed water that can desorb at high temperatures;

- The framework has a negative charge, due to the presence of [AlO<sub>4</sub>] tetrahedra;

This charge can be easily compensated by cations (*i.e.* Na, K, Mg, Ca) in the micropores. Because of their weak bonds, it is possible for ion exchange to take place with other cations in solution and this allows to obtain zeolites with better performances [12-14].

Before the 1940s zeolites were considered materials with no practical use only studied by mineralogists. Natural zeolites have a hydrothermal origin and can easily be found in basaltic and volcanic rocks. 67 different species of zeolites have been identified and classified in nature [11, 15].

Recently, natural zeolites have become very important for the separation and the adsorption of organic compounds or metal ions in the waste treatment field. In fact, zeolites exhibit high thermochemical stability and are able to regenerate themselves easily [16].

Among the natural zeolites, clinoptilolite is one of the most interesting to study. The representative general unit-cell formula is (NaKCa)<sub>4</sub>(Al<sub>6</sub>Si<sub>30</sub>O<sub>72</sub>)·24H<sub>2</sub>O with a void volume, about 34%, estimated from the water content [17, 18]. The water occupies micropores and channels, in which exchangeable cations take

\*Address correspondence to this author at the Department of Applied Science and Technology, Politecnico di Torino, Corso Duca degli Abruzzi 24, 10129 Turin, Italy; Tel: +390110904753; Fax: +390110904624; E-mail: marco.piumetti@polito.it

place: Na, K, Ca or others (Mg, Fe, Sr, Ba) depending on which geographical area the clinoptilolite comes from [17, 19]. The ratio Si/Al can vary from 4.0 to 5.3, according to the Lowenstein's rule: the ratio Si/Al is always larger than 1 [20].

Clinoptilolite can be characterized by different porosities: microporosity (<2 nm), mesoporosity (between 2 and 50 nm) and macroporosity (above 50 nm). The macroporosity is created by the presence of specific mineral (*i.e.* Quartz or Mordenite) [17]. The cation exchange capacity of the clinoptilolite, namely CEC, is about  $2.25 \text{ m}_{\text{equiv}} \text{ g}^{-1}$ . Despite its lower value compared to other natural zeolites (*i.e.* Analcime =  $4.54 \text{ m}_{\text{equiv}} \text{ g}^{-1}$ , Chabazite =  $3.84 \text{ m}_{\text{equiv}} \text{ g}^{-1}$ ), clinoptilolite has an affinity with ions in this increasing order [18]:  $\text{Li} < \text{Mg} < \text{Al} < \text{Fe} < \text{Ca} < \text{Na} < \text{Sr} < \text{Ba} < \text{NH}_4 < \text{K} < \text{Rb} < \text{Cs}$ .

Clinoptilolite is able to exchange its ions with nitrogen from  $[\text{NH}_4]^+$  and with metal ions in aqueous solution [18, 21, 22]. For this reason, clinoptilolite is widely used in the agricultural field as a slow-release nitrogen fertilizer and in the treatment of contaminated water [21-27]. Other interesting studies show how clinoptilolite is used in the treatment of nuclear wastewater in the presence of cadmium and strontium [28-30].

In wastewater treatment the first perception of the quality of the water is its colour. It is estimated that less than 1 ppm for some dyes is visible in water: this value is undesirable [31, 32]. The synthetic dyes are common and widely use in the industries: about  $7 \times 10^5$  tonnes per year are produced and over 100,000 are commercially available [33, 34]. The problem of wastewater from industries is the presence of organic molecules. These molecules react with difficulty: they are stable to light, show aerobic digestion and oxidizing agent and heat [35, 36]. It is estimated that 2% of dyes produced are discharged directly into the blow-down system [32, 34].

Among these dyes, methylene blue (MB) was studied. The physico-chemical properties of clinoptilolite were analyzed by complementary techniques: XRD, physisorption of  $\text{N}_2$  at  $-196 \text{ }^\circ\text{C}$ , field emission scanning electron microscopy (FESEM) and energy dispersive X-ray analysis (EDX).

Then, the adsorption tests were performed with two different solutions of MB at 250 and  $500 \text{ mg L}^{-1}$  with a certain quantity of clinoptilolite (5 g).

## 2. MATERIALS AND METHODS

### 2.1. Physico-Chemical Characterizations

The powder X-ray diffraction patterns were collected on an X'Pert Philips PW3040 diffractometer using  $\text{Cu K}\alpha$  radiation ( $2\theta$  range =  $5^\circ$ – $50^\circ$ ; step =  $0.05^\circ$   $2\theta$ ; time per step = 0.2 s). The diffraction peaks were indexed according to the Powder Data File database (PDF-2 1999, International Centre of Diffraction Data, PA, USA).

The specific surface area ( $S_{\text{BET}}$ ) and total pore volume ( $V_p$ ) were measured by means of  $\text{N}_2$  physisorption at  $-196 \text{ }^\circ\text{C}$  (Micromeritics Tristar II 3020, v1.03, Micromeritics Instrument Corp., Norcross, GA, USA, 2009) on samples previously outgassed at  $200 \text{ }^\circ\text{C}$  for 4 h. This phase is necessary to eliminate adsorbed molecules on the zeolite surface (*i.e.*  $\text{H}_2\text{O}$ ). The specific surface area of the samples was calculated using the Brunauer-Emmett-Teller (BET) method. The pore distribution and the average pore width were studied by Barrett-Joyner-Halenda (BJH) analysis.

The morphology of the samples and the EDX analysis were investigated by means of field emission scanning electron microscopy (FESEM Zeiss MERLIN, Gemini-II column, Oberkochen, Germany).

### 2.2. Adsorption Tests

Two solutions with a concentration of MB of 250 and  $500 \text{ mg L}^{-1}$  were prepared. Then 5 g of clinoptilolite were added to these solutions and mixed at room temperature under constant stirring conditions. The MB adsorption started when the clinoptilolite was added in the solution (time 0). 5 ml of the solution were analyzed over the time (namely, 10, 20, 30, 40, 60, 90, 100, 120 and 130 minute) with a UV-VIS spectroscope using the absorbance of the peak at 664 nm as a reference. Prior to adsorption tests, a calibration curve was created with  $10 \text{ mg L}^{-1}$  of MB.

## 3. RESULTS AND DISCUSSION

### 3.1. Physico-Chemical Characterizations

Figure 1 shows the XRD diffractogram of the clinoptilolite in comparison with the reference code of clinoptilolite itself Figure 1a and the reference of Mordenite, Figure 1b. In Figure 1a it is possible to see the high crystallinity of the clinoptilolite and its more intensive peaks at  $2\theta = 9.92^\circ$ ,  $22.43^\circ$  and

30.50°, according to the literature and the reference code in the database (reference code of the clinoptilolite: 00-039-1383) [37]. It is possible to have several minerals in the clinoptilolite, such as  $\alpha$ -Quartz and Mordenite [37]. In Figure 1b there is the reference code of Mordenite. At  $2\theta = 25.8^\circ$  the diffractogram of clinoptilolite has a reflection peak of the Mordenite. We have compared the code of  $\alpha$ -Quartz (reference code: 01-085-1054) to the clinoptilolite and we noticed there were no traces of quartz in the clinoptilolite (not reported for brevity).

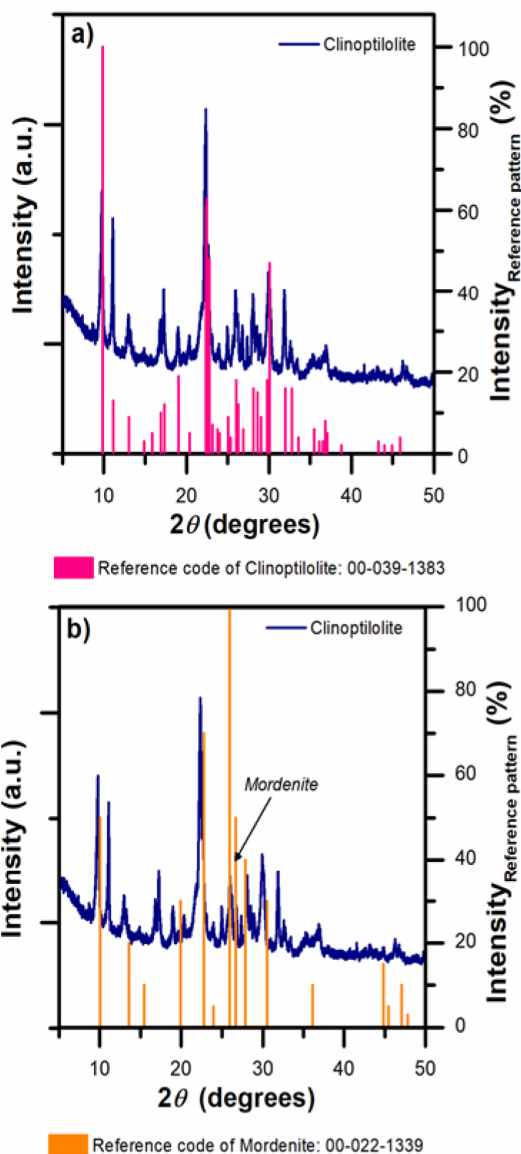


**Figure 1:** XRD diffractograms of clinoptilolite. A comparison with the reference pattern in the database for: **1a)** clinoptilolite and **1b)** mordenite.

At  $2\theta = 22.4^\circ$  there is the most intense peak of the clinoptilolite. The latter is indicated by the (1 3 2) and (0 0 4)-type planes of clinoptilolite [37].

In Table 1 the main textural properties of the clinoptilolite are reported. As a whole, the specific surface area (evaluated by the BET method) and the total pore volume are very low, equal to  $36\text{ m}^2\text{ g}^{-1}$  and  $0.14\text{ cm}^3\text{ g}^{-1}$  respectively.

**Table 1: Textural Properties of the Clinoptilolite**

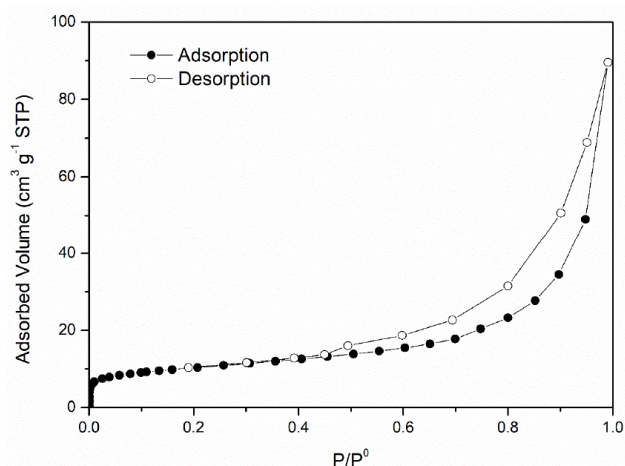
	$S_{\text{BET}} (\text{m}^2\text{ g}^{-1})^1$	$V_p (\text{cm}^3\text{ g}^{-1})^2$	$D_p (\text{nm})^3$
<b>Clinoptilolite</b>	36	0.14	15

<sup>1</sup> Specific surface area measured by the Brunauer-Emmett-Teller (BET) method;

<sup>2</sup> Total pore volume at  $p/p_0 = 0.97$ ;

<sup>3</sup> Average pore width evaluated from BJH method in the desorption phase;

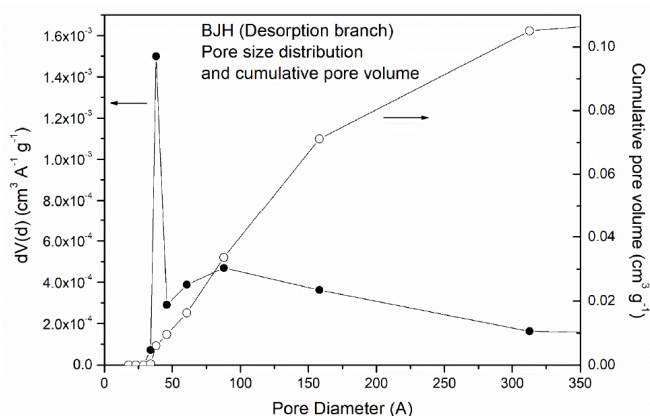
In Figure 2 the adsorption and desorption isotherms of the clinoptilolite are reported. It is possible to evaluate the type of isotherm. As shown in literature, this is a type-IV isotherm that is common among mesoporous materials. The capillarity condensation is accompanied by hysteresis: this phenomena occurs when a critical width is exceeded, in the case of nitrogen the hysteresis starts for pores wider than 4 nm [38, 39]. It is possible to evaluate the shape of the pore by analysis of the hysteresis loop. Hysteresis is a phenomenon which appears during a certain range in the multilayer physisorption and is associated with the capillarity condensation into the pores [38]. The loop does not exhibit limiting adsorption at high relative pressure and the shape is common with plate-like particles that give rise to slit-shaped pores [38].



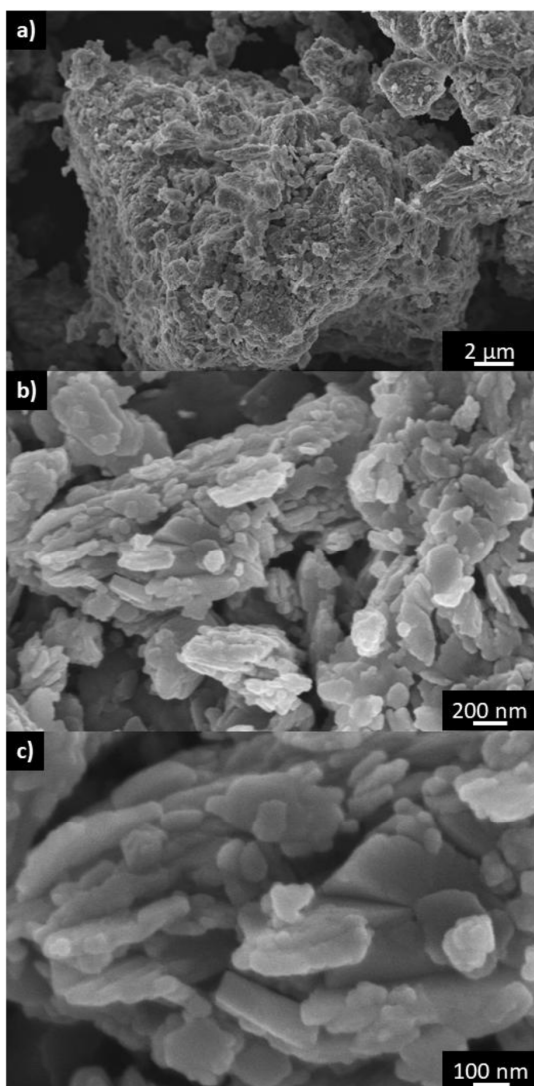
**Figure 2:** Adsorption and desorption isotherms for the clinoptilolite ( $\text{N}_2$ -physisorption at  $-196^\circ\text{C}$ ).

Figure 3 displays pores size distributions of the clinoptilolite during desorption, evaluated by the BJH method. From the desorption phase it possible to evaluate the average diameter of the clinoptilolite pores: this value corresponds to 15 nm.

The distribution does not reach zero. As shown in Figure 3, there is a macroporous region at higher values, between 50 and 120 nm.



**Figure 3:** Pore size distribution of the clinoptilolite.



**Figure 4:** FESEM images of the clinoptilolite at different magnifications: 2  $\mu\text{m}$  a), 200 nm b) and 100 nm c).

In Figure 4 the FESEM micrographs of the clinoptilolite are shown at three different magnification levels: **4a)** at 2  $\mu\text{m}$ , **4b)** at 200 nm and **4c)** at 100 nm.

It seems to have anhedral particles assembled on the top of one other [40]. A rock with this peculiarity has grain with no well-defined crystal faces. Probably during the consolidation of the fuses mass (magma), the initial phases of the zeolite did not crystallize and the crystal growth began in an environment with no free space for the formation of these crystal facets. For this reason, clinoptilolite takes the shape of the free-space made by the minerals that segregated previously. As is shown by Figure 1, in the diffractogram of clinoptilolite, the mordenite is present as an impurity. In literature, the FESEM micrograph of clinoptilolite shows this impurity in filiform shape, crisscrossed among the clinoptilolite plates [40]. However, the clinoptilolite used in the present study does not have this filiform shape in its structure: this means that there is not enough mordenite to be organized in this shape, though there is trace evidence of mordenite because the XRD diffractograms shows its presence in the structure of our clinoptilolite.

In Table 2 the EDX results of the chemical composition of the clinoptilolite are reported.

**Table 2: Chemical Composition of the Clinoptilolite Performed by EDX Analysis**

Element	Atomic (%) <sup>1</sup>
O	55.81 $\pm$ 20.78
Si	31.71 $\pm$ 16.02
Al	6.45 $\pm$ 3.62
K	3.22 $\pm$ 4.47
Ca	1.57 $\pm$ 2.44
Fe	0.68 $\pm$ 1.18
Mg	0.48 $\pm$ 0.09
Na	0.12 $\pm$ 0.40
Tot.	100.00

<sup>1</sup> Values reported with their deviation standard.

As previously stated, clinoptilolite has the generic chemical formula  $(\text{NaKCa})_4(\text{Al}_6\text{Si}_{30}\text{O}_{72})\cdot 24\text{H}_2\text{O}$  [17]. In the present case, the amounts of Na, K and Ca are quite different from each other: clinoptilolite is not homogeneous in terms of composition. During its formation from the magma, the self-assembly of the clinoptilolite is performed in an anisotropic way, so it is

possible to have regions with different composition of element. For this analysis, we used four areas and mediated the values obtained: in this way it is possible to be sure of the real chemical composition of the clinoptilolite.

We also have other elements, such as Fe (0.68% at.) and Mg (0.47% at.): these two are probably the impurities that were enclosed in the pores of the clinoptilolite during its formation from the magma. To confirm these values, we performed the ICP analysis: the results show Fe 0.28 at. % and Mg 0.5 at. %.

### 3.2. Adsorption Tests

In Table 3 the results of the adsorption tests over the MB solution (250 mg L<sup>-1</sup>) with 5 g of clinoptilolite are reported. "F" is the dilution factor used during the experiment. "C<sub>analysis</sub>" is the concentration evaluated using the intercept and the slope values from the calibration curve using the Equation (1):

$$x = \frac{y}{m} - C \quad (1)$$

where both "m" and "C" are known by the calibration curve (not reported for brevity). "C<sub>t</sub>" is the real concentration at the time given and it is evaluated by Equation (2):

$$C_t = C_{analysis} \cdot F \quad (2)$$

where "F" is the dilution factor reported in Table 3.

In Table 3 there is the "q<sub>t</sub>" which is the quantity of MB in mg absorbed per grams of clinoptilolite and it is evaluated as shown by Equation (3):

$$q_t = \left(1 - \frac{C_t + 1}{C_t}\right) \cdot C_{t=0} \cdot \frac{mass_{zeolite}}{volum_{solution}} \quad (3)$$

where the mass is 5 g and the volume of the solution used is 0.5 L.

The results are shown in Figure 5. In Figure 5a it is possible to see that clinoptilolite is a material that can easily adsorb MB in about 20 minutes.

The MB adsorption can be evaluated by a first or a second order reaction. The kinetic order of MB adsorption on clinoptilolite can be calculated via the kinetic constant in both cases (first or second order reaction).

For the first order reaction the Equation (4):

$$-\frac{dc_t}{dt} = k_1 C_t \quad (4)$$

Is used, where k<sub>1</sub> is the kinetic constant for the first order reaction. Integrating with C<sub>t</sub>=C<sub>0</sub> at t=0 it is possible to know the k<sub>1</sub> as the slope of the linear fitting in Figure 6a.

For the second order reaction the Equation (5):

$$-\frac{dq_t}{dt} = k_2 (q_e - q_t)^2 \quad (5)$$

**Table 3: Results of the Absorbance Tests over the Solution 250 mg L<sup>-1</sup> of MB with 5 g of Clinoptilolite**

Time (min)	F	A	C <sub>analysis</sub> (mg L <sup>-1</sup> )	C <sub>t</sub> (mg L <sup>-1</sup> )	Conversion (%)	q <sub>t</sub> (mg g <sup>-1</sup> )
0				250.00	0.0	0.0
10	20	0.168	0.94	18.71	92.5	23.1
20	20	0.154	0.85	16.92	93.2	23.3
30	20	0.133	0.71	14.24	94.3	23.6
40	2	1.135	7.12	14.23	94.3	23.6
60	2	1.13	7.08	14.17	94.3	23.6
70	2	1.002	6.27	12.53	95.0	23.7
80	2	0.96	6.00	12.00	95.2	23.8
90	2	0.92	5.74	11.48	95.4	23.9
100	2	0.857	5.34	10.68	95.7	23.9
120	2	0.835	5.20	10.40	95.8	24.0
130	1	1.59	10.02	10.02	96.0	24.0

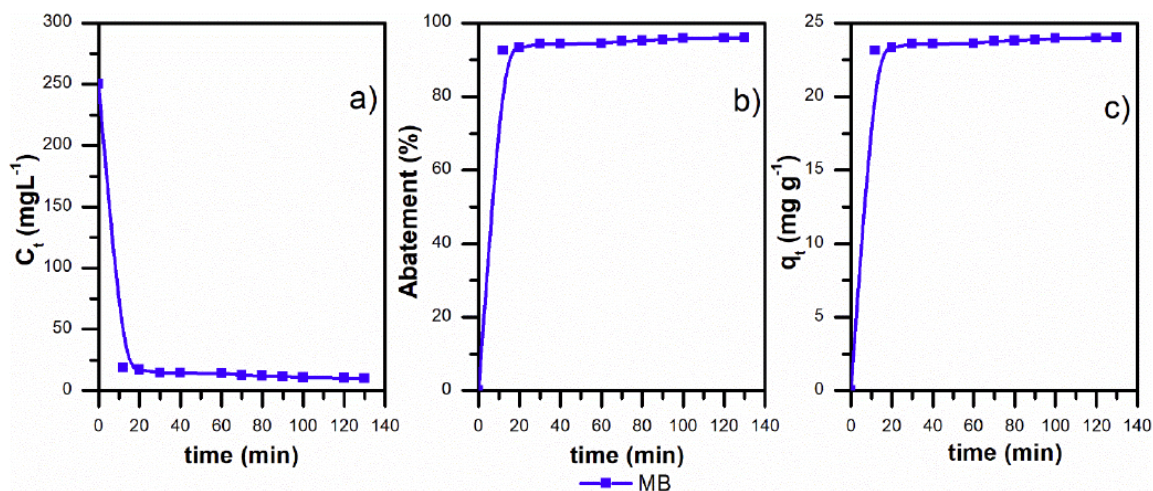


**Figure 5:** Concentration, abatement and quantity of MB absorbed as function of the time for the solution 250 mg L<sup>-1</sup>.

It is used where  $k_2$  is the kinetic constant for the second order reaction.  $q_e$  is the quantity of MB adsorbed per unit mass of clinoptilolite at the equilibrium point and  $k_2$  is the slope of the linear fitting in Figure 6b.

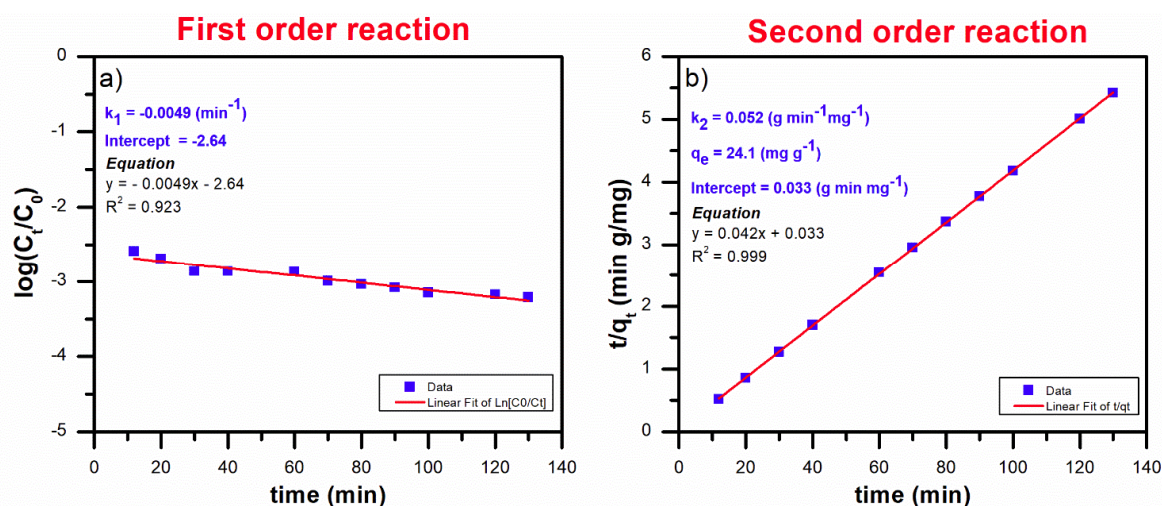
In Figures 6a and 6b the main information about data fitting is reported. For the first order reaction, Figure 6a, the R-square value is about 0.923. For the second order reaction this value is the nearest to 1, about 0.999. This is the discriminating parameter that allows us to find the reaction order. If the R-square is near to one, the fitting was done very well and the reaction order is acceptable. In this study the MB adsorption on clinoptilolite can be described by a second order reaction. Another interesting result of the second order reaction is the  $q_e$ : this value, in ideal

conditions, should be about 25 mg g<sup>-1</sup>. In this study is about 24.1 mg g<sup>-1</sup> and this it is quite near to ideal conditions.

The same procedure is used to evaluate the adsorption of a higher MB concentration, about 500 mg L<sup>-1</sup>. The conditions used are the same as the solution at 250 mg L<sup>-1</sup>.

Table 4 contains the results of the adsorption test for 500 mg L<sup>-1</sup> of MB whereas Figure 7 shows the results of the linear fitting.

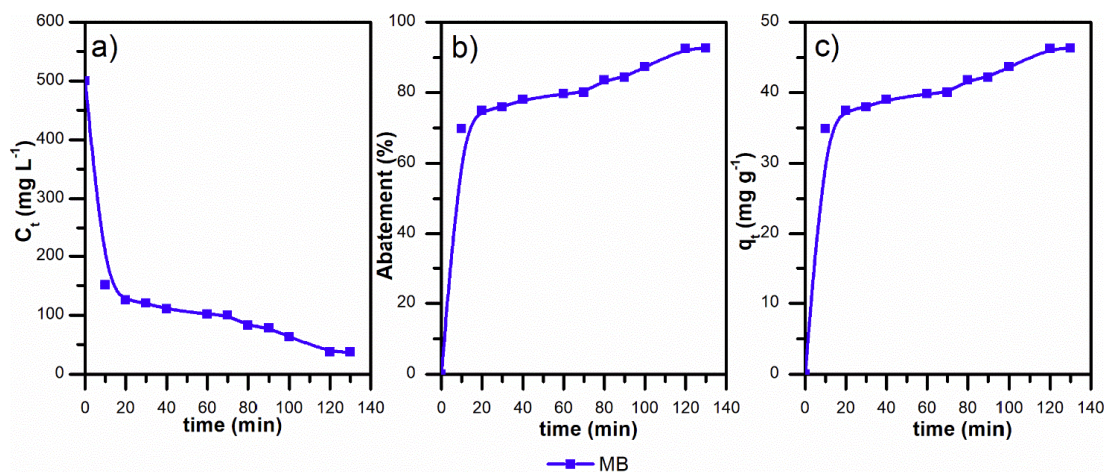
At the same operative conditions, there are differences in the adsorption of MB at different concentrations. It seems that at higher concentrations, difficulties arise for MB to be adsorbed by clinoptilolite.



**Figure 6:** The adsorption of MB (250 mg L<sup>-1</sup>) in the case of a first order reaction 6a) and the second order reaction 6b).

**Table 4: Results of the Absorbance Tests over the Solution 500 mg L<sup>-1</sup> of MB with 5 g of Clinoptilolite**

Time (min)	F	A	C <sub>analysis</sub> (mg L <sup>-1</sup> )	C <sub>t</sub> (mg L <sup>-1</sup> )	Conversion (%)	q <sub>t</sub> (mg g <sup>-1</sup> )
0				500.00		
10	20	1.206	7.57	151.40	69.7	34.9
20	20	1.003	6.27	125.45	74.9	37.5
30	20	0.964	6.02	120.47	75.9	38.0
40	20	0.883	5.51	110.11	78.0	39.0
60	20	0.815	5.07	101.42	79.7	39.9
70	20	0.804	5.00	100.01	80.0	40.0
80	20	0.667	4.13	82.50	83.5	41.7
90	20	0.635	3.92	78.41	84.3	42.2
100	20	0.516	3.16	63.20	87.4	43.7
120	2	2.97	18.85	37.69	92.5	46.2
130	2	2.95	18.72	37.44	92.5	46.3

**Figure 7:** Concentration, abatement and quantity of MB adsorbed as function of the time for the solution 500 mg L<sup>-1</sup>.

As shown in Figure 7a, before 60 minutes, there seems to be a plateau and, after 60 minutes, the concentration of dye decreases. This behaviour is not exhibited in the case of 250 mg L<sup>-1</sup>, Figure 6a. When working with 500 mg L<sup>-1</sup>, there is a higher quantity of dye in solution and the adsorption process is influenced by this parameter: it seems there are difficulties for MB to be adsorbed by the zeolite. This aspect can be explained by the presences of micro and mesopores. The dye molecules, before they diffuse into the pores of clinoptilolite, should cross the boundary layer. If lots of dye molecules are present in solution, this first step is kinetically predominant and in the first minutes of the adsorption, the percentage of abatement is slower. When the molecules diffuse into the pores, the abatement proceeds more quickly [41].

In Figure 7 an overview of the data fitting for the first order (Figure 7a) and the second order reaction (Figure 7b). In Figure 7a is reported, the R-square value is about 0.903. For the second order reaction this value is about 0.991. So, with a concentration of 500 mg L<sup>-1</sup> the adsorption is a second order reaction.

If we compare the kinetic constant of the second order reaction of the two cases reported in Figure 6 and 7, the  $k_2$  of the solution 500 mg L<sup>-1</sup> is about the half of the  $k_2$  of the solution 250 mg L<sup>-1</sup>. This is interesting because the kinetic of the adsorption is influenced by the quantity of the dye in solution.

In other words, if the MB concentration increases, then the adsorption rate decreases.



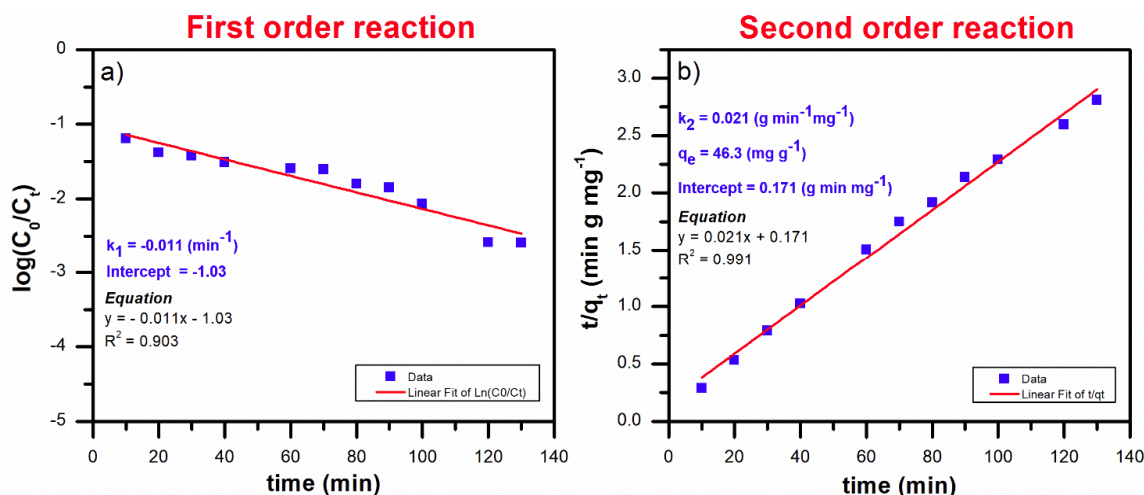


**Figure 8:** The adsorption of MB (500 mg L<sup>-1</sup>) in the case of a first order reaction **a)** and the second order reaction **b)**.

For the solution 500 mg L<sup>-1</sup>, the  $q_e$  is about 46.3 mg g<sup>-1</sup>. This value is not near the ideal one, that is 50 mg g<sup>-1</sup>. This is because this  $q_e$  is related to the capacity of the zeolite to adsorb the dye. As explained above, a higher concentration of MB influences the capacity of adsorption of the clinoptilolite and, at the end of the test, the total quantity adsorbed and the value at the equilibrium condition.

## CONCLUSION

In this work, clinoptilolite was investigated. The X-ray diffractogram confirmed the presence of impurities (mordenite) that are incorporated into the zeolite framework.

This clinoptilolite exhibits low surface area (36 m<sup>2</sup>g<sup>-1</sup>) and pore volume (0.14 cm<sup>3</sup> g<sup>-1</sup>) and the average diameter is 15 nm.

The structure of clinoptilolite was investigated by FESEM micrography: the material has anhedral particles assembled on the top of one other. This kind of shape is the result of a self-assembly of the initial phases of clinoptilolite that do not crystallize.

The EDX analysis revealed the presence of Fe and Mg as impurities (Fe 0.28 at. % and Mg 0.5 at. %)

In order to evaluate the adsorption capacity, the adsorption tests were performed with two solutions of MB (250 and 500 mg L<sup>-1</sup>). The results showed the adsorption is more efficient in the case of 250 mg L<sup>-1</sup>, about 96 % after 2h. For the solution 500 mg L<sup>-1</sup> the abatement is about 92.5% after 2h. The kinetic order of MB adsorption was evaluated and the results suggest a second order reaction.

## ACKNOWLEDGMENT

The study reported in this paper is part of the research project RheoCom “Rheology of complex materials containing nano-sized components for civil engineering applications” carried out in collaboration with Purde University and funded by Politecnico di Torino and Compagnia di SanPaolo, Turin, Italy.

Support of Zeolardoin providing the clinoptilolite used through the investigation is gratefully acknowledged.

The authors thank Marco Armandi for performing the N<sub>2</sub> physisorption measurements and Camilla Galletti, for performing the ICP analysis (Department of Applied Science and Technology, Politecnico di Torino).

## REFERENCES

- [1] Venuto PB. Organic catalysis over zeolites: A perspective on reaction paths within micropores, *Microporous Materials*. Elsevier 1994; 2: 297-411. Available from: <http://www.sciencedirect.com/science/article/pii/0927651394000026>
- [2] Davis ME. Proceedings of the 1997 International Symposium on Zeolites and Microporous Crystals, ZMPC, *Microporous and Mesoporous Materials*. Elsevier 1998; 21: 173-716. Available from: <http://www.sciencedirect.com/science/article/pii/S1387181198000079>
- [3] Tanabe K. Industrial application of solid acid–base catalysts. *Appl Catal A Gen*, Elsevier 1999; 181(2): 399-434. Available from: <http://www.sciencedirect.com/science/article/pii/S0926860X98003974>
- [4] Bein T. Chapter 18 Host-guest interactions in zeolites and periodic mesoporous materials. *Stud Surf Sci Catal*, Elsevier 2007; 168: 611-XIX. Available from: <http://www.sciencedirect.com/science/article/pii/S0167299107808068?via%3Dihub>

- [5] Yilmaz B, Sacco A, Deng J. Electrical transport through monatomic titania chains. *Appl Phys Lett*, American Institute of Physics 2007; 90(15): 152101. Available from: <http://aip.scitation.org/doi/10.1063/1.2720742>
- [6] Sakaguchi K, Matsui M, Mizukami F. Applications of zeolite inorganic composites in biotechnology: Current state and perspectives, Vol. 67, *Applied Microbiology and Biotechnology*. Springer-Verlag 2005; p. 306-11. Available from: <http://link.springer.com/10.1007/s00253-004-1782-4>
- [7] Cronstedt AF. K. Sven. Vetenskapsakad. Handl. K Sven Vetenskapsakad Handl 1756; 17: 120.
- [8] Taylor WH. I. The structure of analcite (NaAlSi<sub>2</sub>O<sub>6</sub>·H<sub>2</sub>O). *Zeitschrift für Krist - Cryst Mater*, De Gruyter Oldenbourg 1930; 74(1-6): 1-19.
- [9] Pauling L. The Structure of Some Sodium and Calcium Aluminosilica Tes. *Proc Natl Acad Sci U S A* 1930; 16: 453. <https://doi.org/10.1073/pnas.16.7.453>
- [10] Pauling L. *Kristallgeometric Kristallphys*. Z Krist 1930; 74: 1.
- [11] Čejka J, Morris RE, Nachtigall P. *Zeolites in catalysis: properties and applications* 2017.
- [12] Ćurković L, Cerjan-Stefanović Š, Filipan T. Metal ion exchange by natural and modified zeolites. *Water Res*, Pergamon 1997; 31(6): 1379-82. Available from: <http://www.sciencedirect.com/science/article/pii/S0043135496004113>
- [13] Iwamoto M, Yahiro H, Mine Y, Kagawa S. Excessively copper ion-exchanged ZSM-5 zeolites as highly active catalysts for direct decomposition of nitrogen monoxide. , Vol. 18, *Chemistry Letters*. The Chemical Society of Japan 1989; p. 213-6. Available from: <http://www.journal.csj.jp/doi/10.1246/cl.1989.213>
- [14] Li Y, Armor JN. Selective catalytic reduction of NO<sub>x</sub> with methane over metal exchange zeolites. *Appl Catal B*, Elsevier 1993; 2(2-3): 239-56. Available from: <http://www.sciencedirect.com/science/article/pii/S092633739380051E>
- [15] Wise WS, Colella C. *Handbook of natural zeolites*. Frede Ed Napoli 2013.
- [16] Chmielewska-Horváthová E, Lesný J. Study of sorption equilibria in the systems: Water solutions of inorganic ions - Clinoptilolite. *J Radioanal Nucl Chem Lett*, Kluwer Academic Publishers 1995; 201(4): 293-301. Available from: <http://link.springer.com/10.1007/BF02164048> <https://doi.org/10.1007/BF02164048>
- [17] Tsitsishvili G, Andronikashvili T, Kirov G, Filizova L. *Natural Zeolites*. Ellis Horwood, New York 1992.
- [18] Mumpton FA. La roca magica: uses of natural zeolites in agriculture and industry. *Proc Natl Acad Sci U S A*, National Academy of Sciences 1999; 96(7): 3463-70. Available from: <http://www.pnas.org/content/96/7/3463.short>
- [19] Mumpton F. Clinoptilolite Redefined. *Am Mineral* 1960; 45: 351-69. Available from: <http://ci.nii.ac.jp/naid/10011941740/>
- [20] Loewenstein W. The distribution of aluminum in the tetrahedra of silicates and aluminates. *Am Mineral* 1954; 39: 92-6. Available from: [http://www.minsocam.org/ammin/AM39/AM39\\_92.pdf](http://www.minsocam.org/ammin/AM39/AM39_92.pdf)
- [21] Vaca Mier M, López Callejas R, Gehr R, Jiménez Cisneros BE, Alvarez PJJ. Heavy metal removal with mexican clinoptilolite: Multi-component ionic exchange. *Water Res*, Pergamon 2001; 35(2): 373-8. Available from: <http://www.sciencedirect.com/science/article/pii/S004313540002700>
- [22] Du Q, Liu S, Cao Z, Wang Y. Ammonia removal from aqueous solution using natural Chinese clinoptilolite. *Sep Purif Technol*, Elsevier 2005; 44(3): 229-34. Available from: <http://www.sciencedirect.com/science/article/pii/S1383586605000493>
- [23] Blanchard G, Maunaye M, Martin G. Removal of heavy metals from waters by means of natural zeolites. *Water Res*, Pergamon 1984; 18(12): 1501-7. Available from: <http://www.sciencedirect.com/science/article/pii/0043135484901246>
- [24] Sprynskyy M, Buszewski B, Terzyk AP, Namieśnik J. Study of the selection mechanism of heavy metal (Pb<sup>2+</sup>, Cu<sup>2+</sup>, Ni<sup>2+</sup>, and Cd<sup>2+</sup>) adsorption on clinoptilolite. *J Colloid Interface Sci*, Academic Press 2006; 304(1): 21-8. Available from: <http://www.sciencedirect.com/science/article/pii/S0021979706006886> <https://doi.org/10.1016/j.jcis.2006.07.068>
- [25] Reháková M, Čuvanová S, Dživák M, Rimár J, Gaval'ová Z. Agricultural and agrochemical uses of natural zeolite of the clinoptilolite type. *Curr Opin Solid State Mater Sci Elsevier* 2004; 8(6): 397-404. Available from: <http://www.sciencedirect.com/science/article/pii/S1359028605000197>
- [26] Perrin TS, Drost DT, Boettinger JL, Norton JM. Ammonium-loaded clinoptilolite: a slow-release nitrogen fertilizer for sweet corn. *J Plant Nutr*, Taylor & Francis Group 1998; 21(3): 515-30. Available from: <http://www.tandfonline.com/doi/abs/10.1080/01904169809365421>
- [27] Lewis MD. *Clinoptilolite, as a N, K, and Zn source for plants*. Colorado State University. Libraries 1981.
- [28] Faghiehian H, Ghannadi Marageh M, Kazemian H. The use of clinoptilolite and its sodium form for removal of radioactive cesium, and strontium from nuclear wastewater and Pb<sup>2+</sup> Ni<sup>2+</sup> Cd<sup>2+</sup> Ba<sup>2+</sup> from municipal wastewater. *Appl Radiat Isot*, Pergamon 1999; 50(4): 655-60. Available from: <http://www.sciencedirect.com/science/article/pii/S0969804398001341>
- [29] Osmanlioglu AE. Treatment of radioactive liquid waste by sorption on natural zeolite in Turkey. *J Hazard Mater*, Elsevier 2006; 137(1): 332-5. Available from: <http://www.sciencedirect.com/science/article/pii/S0304389406001397> <https://doi.org/10.1016/j.jhazmat.2006.02.013>
- [30] Elizondo N V., Ballesteros E, Kharisov BI. Cleaning of liquid radioactive wastes using natural zeolites. *Appl Radiat Isot*, Pergamon 2000; 52(1): 27-30. Available from: <http://www.sciencedirect.com/science/article/pii/S0969804399001104>
- [31] Banat IM, Nigam P, Singh D, Marchant R. Microbial decolorization of textile-dye-containing effluents: A review. *Bioresour Technol* 1996; 58(3): 217-27. [https://doi.org/10.1016/S0960-8524\(96\)00113-7](https://doi.org/10.1016/S0960-8524(96)00113-7)
- [32] Robinson T, McMullan G, Marchant R, Nigam P. Remediation of dyes in textile effluent: A critical review on current treatment technologies with a proposed alternative. *Bioresour Technol*. Elsevier 2001; 77: p. 247-55. Available from: <http://www.sciencedirect.com/science/article/pii/S0960852400000808>
- [33] McMullan G, Meehan C, Conneely A, Kirby N, Robinson T, Nigam P, *et al*. Microbial decolourisation and degradation of textile dyes. *Appl Microbiol Biotechnol* Springer-Verlag 2001; 81-7. Available from: <http://link.springer.com/10.1007/s002530000587>
- [34] Pearce CI, Lloyd JR, Guthrie JT. The removal of colour from textile wastewater using whole bacterial cells: A review. *Dye Pigment*, Elsevier 2003; 58(3): 179-96. Available from: <http://www.sciencedirect.com/science/article/pii/S0143720803000640>
- [35] Sun Q, Yang L. The adsorption of basic dyes from aqueous solution on modified peat-resin particle. *Water Res*, Pergamon 2003; 37(7): 1535-44. Available from: <http://www.sciencedirect.com/science/article/pii/S0043135402005201>

- [36] Ravi Kumar MN V., Rajakala Sridhari T, Durga Bhavani K, Pradip Kumar D. Trends in color removal from textile mill effluents. *Colourage* 1998; 45(8).
- [37] Arcoya A, Gonzalez JA, Travieso N, Seoane XL. scholar. *Clay Miner* 1994; 29: 123-31.
- [38] Sing KSW. Reporting physisorption data for gas/solid systems with special reference to the determination of surface area and porosity (Recommendations 1984). *Pure Appl Chem* 1985; 57(4).
- [39] Piumetti M, Russo N. notes on catalysis for environment and energy, clut, editor. Torino 2017; 208 p.
- [40] Mumpton FA, Ormsby WC. Morphology of zeolites in sedimentary rocks by scanning electron microscopy. *Clays Clay Miner* 1976; 24(1): 1-23.  
<https://doi.org/10.1346/CCMN.1976.0240101>
- [41] Garg VK, Amita M, Kumar R, Gupta R. Basic dye (methylene blue) removal from simulated wastewater by adsorption using Indian Rosewood sawdust: A timber industry waste. *Dye Pigment*, Elsevier 2004; 63(3): 243-50. Available from: <http://www.sciencedirect.com/science/article/pii/S0143720804000518#FIG1>

---

Received on 04-12-2017

Accepted on 26-02-2018

Published on 15-04-2018

<http://dx.doi.org/10.15379/2408-9834.2018.05.01.01>

© 2018 Dosa et al.; Licensee Cosmos Scholars Publishing House.

This is an open access article licensed under the terms of the Creative Commons Attribution Non-Commercial License (<http://creativecommons.org/licenses/by-nc/3.0/>), which permits unrestricted, non-commercial use, distribution and reproduction in any medium, provided the work is properly cited.